

# Design Guidelines for Electronic PMD Equalizers used in Coherent PDM QPSK Systems

N. Mantzoukis<sup>(1)</sup>, A. Vgenis<sup>(1)</sup>, C. S. Petrou<sup>(1)</sup>, I. Roudas<sup>(1)</sup>, T. Kamalakis<sup>(2)</sup>, and L. Raptis<sup>(3)</sup>

<sup>(1)</sup> Dept. of Electrical and Computer Engineering, University of Patras, Rio, Greece, [mantzoukis@ece.upatras.gr](mailto:mantzoukis@ece.upatras.gr)

<sup>(2)</sup> Dept. of Informatics and Telematics, Harokopion University of Athens, Kallithea, Greece, [thkam@hua.gr](mailto:thkam@hua.gr)

<sup>(3)</sup> Formerly with Attica Telecom (currently a self-employed telecom consultant), [lampros.raptis@gmail.com](mailto:lampros.raptis@gmail.com)

**Abstract** We theoretically study the performance of various fractionally-spaced, electronic PMD equalizers in coherent optical PDM QPSK systems using the multicanonical Monte Carlo method. We calculate the required number of equalizer taps for a specific outage probability and different system margins.

## Introduction

Adaptive, blind, multiple input multiple output (MIMO) electronic equalizers are used in coherent optical communications systems to counteract rapid polarization rotations, perform polarization demultiplexing, and combat polarization mode dispersion (PMD) and polarization dependent loss (PDL)<sup>1-4</sup>. However, due to the limited length of their finite impulse response (FIR) filters<sup>1</sup> and singularities in their coefficient adaptation algorithms<sup>3,5</sup>, these equalizers cannot fully eliminate outages even after equalization.

To the best of the authors' knowledge, there is no in depth theoretical study of the performance of these electronic equalizers of various length and coefficient adaptation algorithms in polarization division multiplexed (PDM) quadrature phase-shift keying (QPSK) coherent optical communications systems. This is mainly due to the fact that power outages after electronic equalization can occur very rarely and hence, even experimental measurements may be unable to assess the system performance<sup>2-4</sup>. It is necessary to use importance sampling methods, such as the multicanonical Monte Carlo (MMC)<sup>6</sup> method, in order to reduce the simulation time required to estimate the statistics of these rare events. The simulation can be further accelerated by using parallel programming.

In this paper, we use a parallel implementation of the MMC method for the efficient evaluation of the outage probability of a coherent PDM QPSK system after PMD equalization. We compare the performance of three popular adaptive, PMD electronic equalizers, which are based on the constant modulus algorithm<sup>7</sup> (CMA), the decision-directed least mean square (DD-LMS) algorithm<sup>4</sup>, and their combination<sup>3</sup>, respectively.

It is shown that both CMA and DD-LMS-based PMD equalizers with as few as  $10 T_s / 2$  -

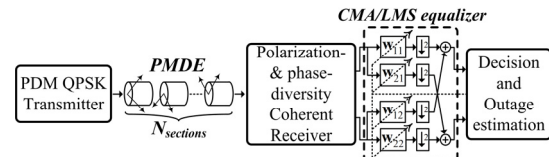


**Fig. 1:** System block diagram (Abbreviations: PMDE: PMD Emulator,  $w$ : Finite Impulse Response (FIR) filters' taps, CMA: Constant Modulus Algorithm, LMS: Least Mean Square).

spaced taps per FIR filter (where  $T_s$  is the symbol period) can reduce the outage probability to less than  $10^{-5}$  for a mean differential group delay (DGD) equal to one symbol period. However, CMA equalizers perform slightly better than the DD-LMS equalizers at links with larger DGD values, whereas the opposite holds true for the low PMD regime. This is the reason why running DD-LMS after a first round of CMA-based equalization provides better performance than using either one of the equalization algorithms alone<sup>3</sup>.

## System model

The block diagram of the coherent PDM QPSK system under study is shown in Fig. 1. In the PDM QPSK transmitter, the two orthogonal polarization components,  $x$ ,  $y$ , of the electric field at the output of a laser source are independently QPSK modulated with non-return-to-zero pulses. Pseudo-random De Bruijn symbol sequences of length  $4^d$  are used, in order to accurately model all possible combinations of  $d$ -symbol-long inter-symbol interference (ISI) caused by PMD.

The PMD emulator is modelled as a concatenation of 30 birefringent waveplates. Each birefringent waveplate is characterized by three random variables,  $\{\alpha_m, \varepsilon_m, \Delta\tau_m\}$ , where  $\{\alpha_m, \varepsilon_m\}$  are the azimuth and ellipticity of the slow principal axis, and  $\{\Delta\tau_m\}$  is the differential group delay, respectively. The statistics of  $\{\alpha_m, \varepsilon_m, \Delta\tau_m\}$

are such that the corresponding instantaneous DGD follows a Maxwellian probability density function (pdf)<sup>8</sup>. For simplicity, PDL, chromatic dispersion and nonlinearities are neglected. Laser phase noise is omitted and it is assumed that the intermediate frequency offset is zero.

A coherent, homodyne, polarization- and phase-diversity receiver is used, consisting of ideal  $2 \times 4$   $90^\circ$  optical hybrids and balanced detectors, followed by 4<sup>th</sup>-order Bessel low-pass filters with  $0.8R_s$  3-dB bandwidth.

PMD compensation and polarization demultiplexing are performed using the aforementioned adaptive MIMO electronic equalizers. They have a butterfly structure consisting of four transversal FIR filters, whose impulse responses are denoted in Fig. 1 by  $\mathbf{w}_{ij}$ ,  $i,j=2$ . Feed-forward frequency and phase-error estimators are used<sup>2</sup>, to remove any small residual constellation rotations.

The PMD-induced OSNR penalty is defined as the difference in OSNR between the back-to-back case and after transmission, required to achieve an error probability of  $10^{-9}$ . The outage probability is defined as the probability that the OSNR penalty exceeds a specified system margin. The outage probability must be below a desirable level<sup>8</sup>, e.g.,  $10^{-5}$ .

#### Multicanonical Monte Carlo method

In our simulations, the statistics of the random variables,  $\{\alpha_m, \varepsilon_m, \Delta\tau_m\}$ , are iteratively biased using the MMC method<sup>6</sup> in order to artificially generate outages. The output random variable is the OSNR penalty, whose pdf is unknown. During each iteration of the MMC algorithm, several fiber realizations, corresponding to different sets of the input random variables  $\{\alpha_m, \varepsilon_m, \Delta\tau_m\}$  are generated based on a random walk in the space of  $\{\alpha_m, \varepsilon_m, \Delta\tau_m\}$ <sup>6</sup>. The corresponding OSNR penalty values are calculated and their histogram is constructed. During the next iteration, the information of the estimated OSNR penalty histogram is used to bias the input joint pdfs, in order to force more samples to fall on the tails of the desired output pdf.

The novelty here is that parallel programming is used to reduce simulation time. Parallelization is performed in two ways: First, embarrassingly parallel simulation is achieved by launching concurrently simulation jobs, corresponding to different mean DGD values, to different multicore computers. Second, individual simulation jobs are accelerated by using the command “parfor” of parallel Matlab. The latter can decrease the execution time for each separate MMC simulation up to three times using four cores of a Quad Intel processor.

#### Results and Discussion

A qualitative comparison of the performance of the aforementioned electronic equalizers is shown in Fig. 2 (a), (b). In the upper row of Fig. 2 (a), (b), constellation diagrams for the “uncompensated case” are shown. This is the case when a CMA-based polarization demultiplexer with a single  $T_s$ -spaced tap per FIR filter is used instead of a PMD equalizer. The second row of Fig. 2 (a), (b) shows constellation diagrams after various equalizers. These results illustrate our claim that CMA equalizers perform better than the DD-LMS equalizers at high PMD regime, contrary to the low PMD regime, where DD-LMS equalizers are superior. We observe that the successive application of CMA- and DD-LMS-based equalization offers better performance compared to either stand-alone equalizers, under the same PMD conditions.

Subsequently, the outage probability after equalization is evaluated as a function of normalized mean DGD, using different system margins. The results are shown in Fig. 3 (a) and (b) for the CMA-based and for the LMS-based equalizer, respectively.

It is worth noting that CMA-based equalizers are more robust than their DD-LMS counterparts in the presence of high PMD. For instance, CMA-based equalizers with 20  $T_s/2$ -spaced taps per FIR filter can compensate for a mean DGD  $1.8T_s$  at an outage probability of  $10^{-5}$  and for a 1-dB system margin [Fig. 3(a)]. On the contrary, similar DD-LMS equalizers can compensate only for a mean DGD  $1.52T_s$  under the same conditions [Fig. 3(b)]. Therefore, use of CMA-based equalizers leads to a 18.4%

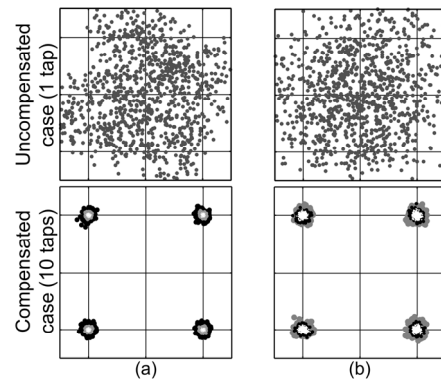


**Fig. 2:** Constellation diagrams for a normalized instantaneous DGD (a) of  $0.64T_s$  (low PMD) and (b) of  $2.25T_s$  (high PMD). Upper row: uncompensated case (1-tap CMA-based polarization demultiplexer). Lower row: after an equalizer with 10  $T_s/2$ -spaced taps. (Symbols: grey points: DD-LMS; black points: CMA; white points: CMA/LMS).

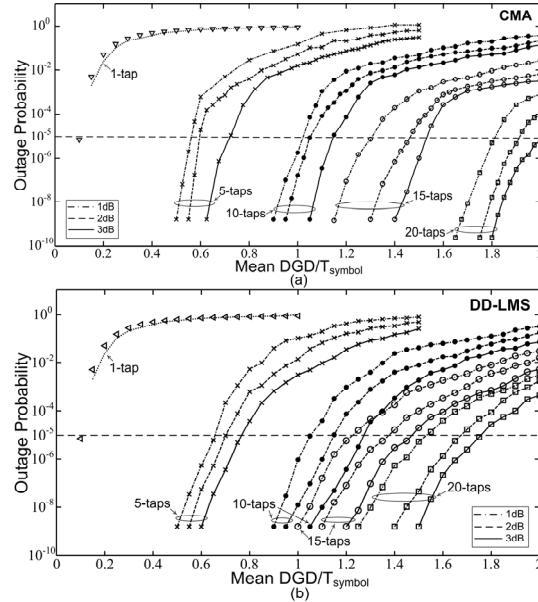


**Fig. 3:** Outage probability as a function of the normalized mean DGD. (a) CMA-based equalizer; (b) DD-LMS-based equalizer. (Symbols: dotted line: 1-tap polarization demultiplexer; triangles: theoretical prediction using Antonelli's model<sup>9</sup>; crosses: 5-taps; filled circles: 10-taps; open circles: 15-taps; squares: 20-taps; dash-dot line: 1-dB margin; dashed line: 2-dB margin; solid line: 3-dB margin).

increase of the acceptable mean DGD or, equivalently, to a 40.2% longer transmission distance.

However, the opposite holds true for the low PMD regime. For instance, CMA-based equalizers with 5 taps can compensate for a mean DGD  $0.58T_s$  [Fig. 3 (a)], as opposed to  $0.65T_s$  for their LMS-based counterparts at an outage probability of  $10^{-5}$  and a system margin of 1 dB [Fig. 3(b)].

Furthermore, in Fig. 3 (a) and (b), if the PMD margin is relaxed from 1 dB to 3 dB, the acceptable mean DGD increases significantly, for both equalizer types. For instance, it is possible to achieve a 36.7% longer transmission distance for a 15-tap CMA-based equalizer, at an outage probability of  $10^{-5}$ . This figure increases to 47.2% for a 15 tap DD-LMS-based equalizer under the same conditions.

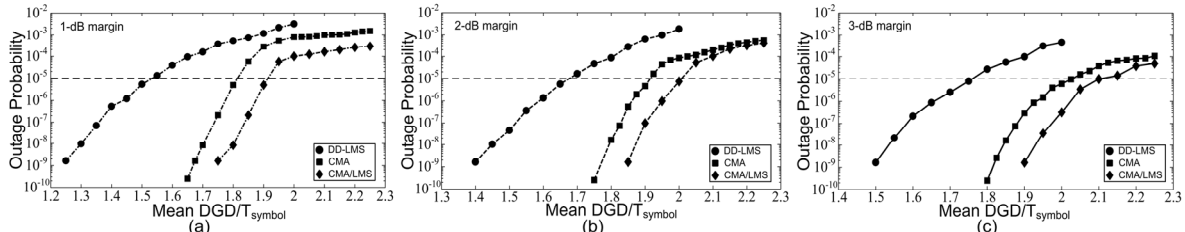


**Fig. 4:** Outage probability as a function of the normalized mean DGD. (a) 1-dB margin; (b) 2-dB margin; (c) 3-dB margin. (Symbols: filled circles: 20-taps DD-LMS-based equalizer; filled squares: 20-taps CMA-based equalizer; diamonds: 20-taps CMA/LMS-based equalizer).

Finally, Fig. 4 compares the performances of stand-alone CMA-based and DD-LMS-based equalizers with  $20 T_s / 2$ -spaced taps per FIR filter against their combination. Simulations show that the latter can tolerate a 6.67% more mean DGD than the conventional CMA-based equalizer at an outage probability of  $10^{-5}$  and for 1-dB margin.

## Conclusions

In this paper, we compared the performance of fractionally-spaced, CMA-, DD-LMS- and CMA/LMS-based PMD equalizers in coherent PDM QPSK systems in the exclusive presence of PMD. The outage probability was used as a performance criterion. Very rare PMD events were generated using a parallel programming implementation of the MMC method. It was shown that CMA equalizers perform slightly better than their DD-LMS counterparts at high PMD regime, whereas the opposite holds true for the low PMD regime. Successive application of these adaptive equalization algorithms offers a better performance than either one alone.

This research project is co-financed by E.U.-European Social Fund (80%) and the Greek Ministry of Development - GSRT (20%).

## References

- 1 C. R. S. Fludger et al., J. Lightwave Technol. **26**, 64 (2008).
- 2 J. Renaudier et al., J. Lightwave Technol. **26**, 36 (2008).
- 3 S. J. Savory, Opt. Express **16**, 804 (2008).
- 4 D. E. Crivelli et al., Proc. GLOBECOM'04, TX (2004).
- 5 I. Roudas et al., J. Lightwave Technol. **28**, 1121 (2010).
- 6 A. Bononi et al., Proc. GLOBECOM'09, CTS-14 (2009).
- 7 S. Haykin, *Adaptive filter theory*, Prentice-Hall, (1996).
- 8 C. D. Poole et al., *Optical Fiber Communication*, Academic Press (1997).
- 9 C. Antonelli et al., Photon. Technol. Lett., **17**, 1482 (2005).